1-Ethyl Gallate-2-Substituted Phenoxymethyl Benzimidazoles: Synthesis, Molecular Structure, Antimicrobial Activities and Complex with Cr(III)

[1, 2]Li Zhao, [1, 2]Guirong Qiu, [1, 2]Jiacheng Wu, [1, 2]Zhiyuan Wang and [1, 2]Haibin Gu*
[1]*Key Laboratory of Leather Chemistry and Engineering of Ministry of Education, Sichuan University, Chengdu 610065, China.*
[2]*National Engineering Laboratory for Clean Technology of Leather Manufacture, Sichuan University, Chengdu 610065, China.*
guhaibinkong@126.com*

(Received on 4th July 2016, accepted in revised form 5th April 2017)

Summary: The design of gallate and benzimidazole containing derivatives is expected to produce new bioactive molecules with multiple applications. Here the synthesis of eight novel benzimidazole compounds containing ethyl gallate and substituted phenoxymethyl units are reported. Firstly, the ring closure reaction between *o*-phenylendiamine and substituted phenoxyacetic acids resulted in 2-substituted phenoxymethyl benzimidazoles that were then modified by the N-hydroxyethylation with 2-chloroethyl alcohol under a phase transfer catalysis condition. The obtained 1-hydroxyethyl-2-substituted phenoxymethyl benzimidazoles were finally translated into the target title compounds **8a-h** by an indirect esterification method in which three O-H groups of gallic acid were first protected by acetyls and deprotected after the esterification reaction by adding hydrazine hydrate. The structures of the title products **8a-h** were fully characterized and confirmed by elemental analysis, MS, IR, ^{1}H-NMR, ^{13}C-NMR and single crystal X-ray diffraction techniques. Antimicrobial tests by inhibition zones indicated that these compounds exhibited diverse inhibitory effects against the test bacteria and fungi, and the type and position of the substituent groups in the phenoxymethyl moieties had obvious influence on their antimicrobial activities. Furthermore, the Cr(III) complex of **8h** was synthesized, and various spectral, elemental and thermal analysis results confirmed that the central Cr(III) atom coordinated with adjacent hydroxyl groups of two **8h** ligands, nitrate and H_2O, respectively.

Keywords: Gallates, Benzimidazole derivatives, Phenoxyacetic acid, Antimicrobial activity, Cr(III) complex.

Introduction

Gallic acid [1], namely, 3, 4, 5-trihydroxybenzoic acid, exhibited many biological, physiological and pharmacological activities, and its derivatives, especially gallates that can be prepared by the esterification reaction with various alcohols, have attracted widely attentions from medical, food, agricultural and industrial communities [2]. In the last decades, considerable reports focused on the synthesis and application of gallate derivatives for their anti-inflammatory [3], anticancer [2], antiarthritic [4], antiviral [5], antibacterial [6, 7], antifungal [6-9], antiangiogenic [10], antioxidative [11, 12], neuroprotective [13], and cholesterol-lowering effects [14].

Also, benzimidazole derivatives are well known for their diverse biological and pharmacological activities such as antimicrobial [15-19], anticancer [20-22], anti-inflammatory [23], antiparasitic [24], antihypertensive [25], anti-HIV [26-28], anticonvulsant [29], antitubercular [26, 28, 30], antioxidant [28, 31], antidiabetic [26, 32], antihistaminic [23, 26, 28] and antimalarial properties [33], and have been used as starting compounds, intermediates or subunits for the development of functional molecules [34]. Modifications of benzimidazole molecule, which can be conducted on the phenyl ring or/and the imidazole ring, provided an important and effective synthetic strategy in the drug discovery process.

In this study, the carbon (or 1) positon in the imidazole ring was modified by the phenoxymethyl units with different substitution groups. Phenoxyacetic acid derivatives showed various bioactivities including antimicrobial [35-39], antiviral [40], antidiabetic [41, 42] and phytohormone effects [43], and as shown in Scheme 1, the ring closure reaction of their carboxyl groups with *o*-phenylendiamine resulted in the compounds **5** containing the two basic structural units of benzimidazole and phenoxymethyl. Then, the N-hydroxyethylation reaction was conducted in the imidazole ring of **5** by using 2-chloroethyl alcohol with the aid of tetrabutyl ammonium bromide (TBAB) as a solid-liquid phase transfer catalyst. Finally, the obtained intermediates **6** containing hydroxyl groups were used to synthesize the target compounds **8** by an indirect esterification protocol in which the three phenolic hydroxyl groups of gallic acid were first protected by acetyls, and

*To whom all correspondence should be addressed.

deprotected after the esterification reaction by using hydrazine hydrate. Thus, the obtained molecules **8** contain three bioactive units, namely, gallate, benzimidazole and phenoxymethyl, and their bioactivities can be adjusted by the type and location of substitute groups in the benzene ring of phenoxymethyl structure. To prove this point, eight compounds **8a-8h** were prepared according to the route in Scheme 1, and their molecular structures were characterized by elementary analysis, MS, IR, ^{1}H-NMR, ^{13}C-NMR and X-ray single crystal diffraction, and the inhibition zone method was adopted to determine their antibacterial and antifungal activities. Furthermore, the Cr(III) complex of **8h**, which has potential applications such as DNA binders [44-45], superoxide radical scavengers[46], cancer chemopreventive agents [47] and tanning agents for collagen and hides [48], was successfully synthesized and well characterized by many techniques containing IR, UV-visible, ^{1}H-NMR, ^{13}C-NMR and TG.

Experimental

All the used reagents were analytic grade, commercially purchased and used as received. All the solvents used were dried and freshly distilled. Trisacetyl-galloyl chloride (**3**) and 1-hydroxyethyl-2-substituted phenoxymethyl benzimidazoles (**6**) and were synthesized according to previous reports [7, 49, 50].

A Shanghai Zhongguang WRS-2 melting point apparatus (uncorrected) was used to determine the melting points of compounds. Elemental analysis (C, H, N) were carried out on a Carlo-Erba 1106 analyser. The infrared spectra were recorded on a Magna. IR 506 (Nicolet Ltd, USA) FT-IR spectrophotometer using KBr disk in the range 4000-400 cm^{-1}. ^{1}H (400 MHz) and ^{13}C-NMR (150 MHz) spectra were recorded at 25 ^{o}C with a Bruker AV II-400 and 600 MHz spectrometer. All the chemical shifts are reported in parts per million (δ, ppm) with reference to tetramethylsilane (TMS). Mass spectra were measured using a GCMS-QP2010 Plus Model GC-MS spectrometer. UV-visible absorption spectra were measured with a Perkin-Elmer Lambda 19 UV visible spectrometer. Thermogravimetric (TG) analysis was conducted on a Netzsch TG 209 F1 thermal analyzer in the range 40-800 ^{o}C with the heating rate of 10 K/min. The measurement of single crystal was carried out on a CCD X-ray single crystal diffractometer (Xcalibur, Eos, UK) with a graphite-monochromated MoKα radiation. A suitable single crystal was selected and mounted on a glass fiber, X-ray diffraction intensity data were collected using the ω-2θ scan technique. The crystal was kept at 293(2) K during data collection. Using Olex2 [51], the structure was solved with the Superflip [52] structure solution program using Charge Flipping and refined with the ShelXL [53] refinement package using Least Squares minimisation.

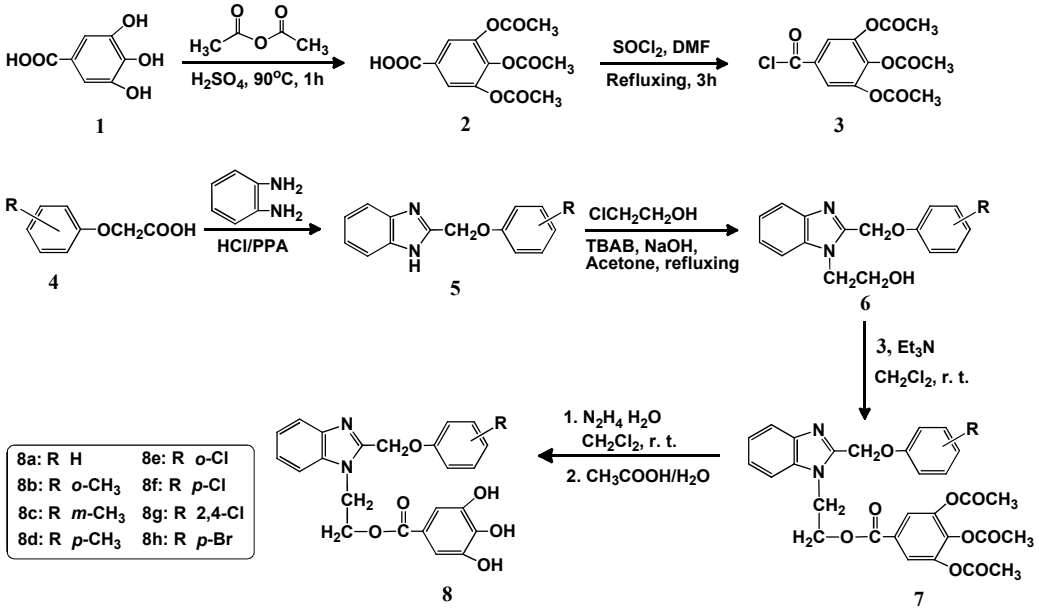

Scheme-1: Synthetic route of 1-ethyl gallate-2-substituted phenoxymethyl benzimidazoles.

Synthesis of **8a:** Trisacetyl galloyl chloride (**3**, 0.3147 g, 1 mmol) was added into a mixture of 1-hydroxyethyl phenoxymethyl benzimidazole (**6a**, 0.2683 g, 1mmol) and triethylamine (0.7 mL, 5 mmol) dissolved in 20 mL dry dichloromethane (CH_2Cl_2) at an ice bath condition. The obtained mixture was stirred for 10 hours at room temperature (r. t., 25 ^oC), then 10 mL of 10% (v/v) HCl was added to remove the excess triethylamine. The CH_2Cl_2 layer was separated and washed with distilled water (3 × 10 mL). The 80% hydrazine monohydrate (0.1878 g, 3 mmol) was then added to the CH_2Cl_2 solution, and the mixture was stirred for 3 hours at r. t. and washed using the 0.3 mol L^{-1} acetic acid solution (10 mL). The formed precipitate was filtered and collected, while the filtrate was separated to remove the water layer. The organic layer was vacuumed, and the obtained residue was combined with the above precipitate and then recrystallized in the mixed solvent of ethanol and distilled water (8:2, v/v) to produce purified 1-ethyl gallate-2-phenoxymethyl benzimidazole (**8a**) as a white solid. Similar procedures were adopted for the synthesis of **8b-8h**. Yield: 85.7%. m. p. 221.5-221.8 ^oC. Anal. calcd. (%) for $C_{23}H_{20}N_2O_6$: C, 65.71; H, 4.76; N, 6.67. Found (%): C, 65.70; H, 4.77; N, 6.65. MS (ESI, *m/z*), calcd. for $C_{23}H_{20}N_2O_6$: 420.41; found: 421.22 ($M+H^+$). ^{1}H-NMR (400 MHz, DMSO-d_6), δ_{ppm}: 9.30 (s, 2H, Ar-OH), 9.04 (s, 1H, Ar-OH), 7.68 (t, 2H, Ar-H), 7.33-7.27 (q, 3H, Ar-H), 7.23 (t, 1H, Ar-H), 7.09(d, 2H, Ar-H), 6.98 (t, 1H, Ar-H), 6.88 (s, 2H, Ar-H), 5.45 (s, 2H, CH_2-O-Ar), 4.72 (t, 2H, N-CH_2), 4.57 (t, 2H, CH_2-OOC-Ar). ^{13}C-NMR (100 MHz, DMSO-d_6), δ_{ppm}: 165.6(**C**OO), 157.7, 149.5(N=**C**-N), 145.6, 141.8, 138.7, 135.4, 129.6, 123.0, 122.1, 121.4, 119.4, 118.7, 114.8, 110.8, 108.7, 63.0(**C**H_2O-Ar), 62.4(**C**H_2OOC-Ar), 42.6(N-**C**H_2). Selected IR (KBr, cm^{-1}): 3519.7, 3384.2 (ν_{OH}), 1718.2 ($\nu_{C=O}$), 1614.7 ($\nu_{C=N}$), 1599.5, 1589.3, 1523.4, 1496.7, 1465.3 ($\nu_{C=C, Ar}$), 1450.5 (δ_{CH2}), 1391.1, 1374.9, 1334.7 (ν_{C-N}), 1310.2, 1232.8 (δ_{OH}), 1205.5 (ν_{Ar-O-C}), 1085.9, 1032.7, 1007.1 (ν_{Ar-O-C}), 896.5, 879.3, 817.0, 765.1, 747.2 (δ_{Ar-H}).

8b: white solid. Yield: 84.1%. m. p. 225.5-225.9 ^oC. Anal. calcd. (%) for $C_{24}H_{22}N_2O_6$: C, 66.35; H, 5.10; N, 6.45. Found (%): C, 66.34; H, 5.02; N, 6.43. MS (ESI, *m/z*), calcd. for $C_{24}H_{22}N_2O_6$: 434.44; found: 435.21 ($M+H^+$). ^{1}H-NMR (400 MHz, DMSO-d_6), δ_{ppm}: 9.30 (s, 2H, Ar-OH), 9.04(s, 1H, Ar-OH), 7.72-7.67 (q, 2H, Ar-H), 7.31 (t, 1H, Ar-H), 7.24 (t, 1H, Ar-H), 7.19-7.14 (m, 3H, Ar-H), 6.90-6.86 (m, 3H, Ar-H), 5.46 (s, 2H, CH_2-O-Ar), 4.76 (t, 2H, N-CH_2), 4.56 (t, 2H, CH_2-OOC-Ar), 2.17 (s, 3H, CH_3). ^{13}C-NMR (100 MHz, DMSO-d_6), δ_{ppm}: 165.6 (**C**OO), 155.8, 149.6 (N=**C**-N), 145.6, 141.6, 138.8, 135.4, 130.7, 127.0, 125.9, 123.1, 122.2, 121.1, 119.3, 118.7, 111.8, 110.9, 108.7, 63.0 (**C**H_2O-Ar), 62.6 (**C**H_2OOC-Ar), 42.6 (N-**C**H_2), 16.0(CH_3). Selected IR (KBr, cm^{-1}): 3515.5, 3463.1 (ν_{OH}), 2961.2 (ν_{CH3}), 1697.3 ($\nu_{C=O}$), 1614.3 ($\nu_{C=N}$), 1540.8, 1524.5 1494.2, 1465.2 ($\nu_{C=C, Ar}$), 1450.2 (δ_{CH3}), 1395.8, 1365.3, 1347.2 (ν_{C-N}), 1316.3, 1236.3 (δ_{OH}), 1216.3 (ν_{Ar-O-C}), 1120.2, 1043.3 1006.5 (ν_{Ar-O-C}), 890.1, 870.3, 849.6, 766.3, 743.4 (δ_{Ar-H}).

8c: white solid. Yield: 81.3%. m. p. 200.1-200.7 ^oC. Anal. calcd. (%) for $C_{24}H_{22}N_2O_6$: C, 66.35; H, 5.10; N, 6.45. Found (%): C, 66.33; H, 5.04; N, 6.48. MS (ESI, *m/z*), calcd. for $C_{24}H_{22}N_2O_6$: 434.44; found: 435.24 ($M+H^+$). ^{1}H-NMR (400 MHz, DMSO-d_6), δ_{ppm}: 9.30 (s, 2H, Ar-OH), 9.04 (s, 1H, Ar-OH), 7.68 (t, 2H, Ar-H), 7.31-7.16 (m, 3H, Ar-H), 6.90-6.88 (m, 4H, Ar-H), 6.79 (d, 1H, Ar-H), 5.41 (s, 2H, CH_2-O-Ar), 4.71 (t, 2H, N-CH_2), 4.57 (t, 2H, CH_2-OOC-Ar), 2.26 (s, 3H, CH_3). ^{13}C-NMR (100 MHz, DMSO-d_6), δ_{ppm}: 165.6 (**C**OO), 157.7, 149.5 (N=**C**-N), 145.6, 141.8, 139.2, 138.7, 135.4, 129.3, 123.0, 122.1, 122.0, 119.4, 118.7, 115.4, 111.7, 110.8, 108.7, 62.9 (**C**H_2O-Ar), 62.4 (**C**H_2OOC-Ar), 42.7 (N-**C**H_2), 21.1(CH_3). Selected IR (KBr, cm^{-1}): 3488.7, 3445.4 (ν_{OH}), 2960.5 (ν_{CH3}), 1722.9 ($\nu_{C=O}$), 1633.4 ($\nu_{C=N}$), 1603.3, 1593.5, 1551.5, 1520.8, 1489.7, 1456.1 ($\nu_{C=C, Ar}$), 1443.6 (δ_{CH3}), 1384.7, 1368.7, 1345.5 (ν_{C-N}), 1298.0, 1259.7, 1225.9(δ_{OH}), 1204.8(ν_{Ar-O-C}), 1169.4, 1045.3, 1036.1, 1004.8 (ν_{Ar-O-C}), 885.0, 847.1, 796.2, 773.2, 761.9, 748.6 (δ_{Ar-H}).

8d: white solid. Yield: 87.7%. m. p. 228.8-229.9 ^oC. Anal. calcd. (%) for $C_{24}H_{22}N_2O_6$: C, 66.35; H, 5.10; N, 6.45. Found (%): C, 66.29; H, 5.01; N, 6.46. MS (ESI, *m/z*), calcd. for $C_{24}H_{22}N_2O_6$: 434.44; found: 435.26 ($M+H^+$). ^{1}H-NMR (400 MHz, DMSO-d_6), δ_{ppm}: 9.29 (s, 2H, Ar-OH), 9.03 (s, 1H, Ar-OH), 7.67 (t, 2H, Ar-H), 7.29 (t, 1H, Ar-H), 7.22 (t, 1H, Ar-H), 7.10 (d, 2H, Ar-H), 6.98 (d, 2H, Ar-H), 6.88 (s, 2H, Ar-H), 5.40 (s, 2H, CH_2-O-Ar), 4.71 (t, 2H, N-CH_2), 4.56 (t, 2H, CH_2-OOC-Ar), 2.22 (s, 3H, CH_3). ^{13}C-NMR (100 MHz, DMSO-d_6), δ_{ppm}: 165.6 (**C**OO), 155.6, 149.6 (N=**C**-N), 145.6, 141.8, 138.7, 135.4, 130.2, 129.9, 123.0, 122.0, 119.4, 118.7, 114.7, 110.8, 108.7, 62.9 (**C**H_2O-Ar), 62.6 (**C**H_2OOC-Ar), 42.6 (N-**C**H_2), 20.1 (CH_3). Selected IR (KBr, cm^{-1}): 3500.9, 3420.3 (ν_{OH}), 2962.2 (ν_{CH3}), 1696.4 ($\nu_{C=O}$), 1416.3($\nu_{C=N}$), 1601.3, 1529.3, 1509.8, 1474.9 ($\nu_{C=C, Ar}$), 1449.0 (δ_{CH3}), 1393.6, 1373.0, 1339.7 (ν_{C-N}), 1310.8, 1229.4 (δ_{OH}), 1210.2 (ν_{Ar-O-C}), 1108.7, 1047.0

1004.1 ($\nu_{Ar\text{-}O\text{-}C}$), 891.0, 872.0, 819.6, 801.8, 770.3, 751.8 ($\delta_{Ar\text{-}H}$).

8e: white solid. Yield: 91.4%. m. p. 234.9-236.1 °C. Anal. calcd. (%) for $C_{23}H_{19}N_2O_6Cl$: C, 60.73; H, 4.21; N, 6.16. Found (%): C, 60.79; H, 4.23; N, 6.14. MS (ESI, *m/z*), calcd. for $C_{23}H_{19}N_2O_6Cl$: 454.86; found: 455.22 ($M+H^+$). ^{1}H-NMR (400 MHz, DMSO-d_6), δ_{ppm}: 9.29 (s, 2H, Ar-OH), 9.03 (s, 1H, Ar-OH), 7.71-7.66 (q, 2H, Ar-H), 7.46-7.22 (m, 5H, Ar-H), 7.00 (t, 1H, Ar-H), 6.87 (s, 2H, Ar-H), 5.57 (s, 2H, CH_2-O-Ar), 4.77 (t, 2H, N-CH_2), 4.59 (t, 2H, CH_2-OOC-Ar). ^{13}C-NMR (100 MHz, DMSO-d_6), δ_{ppm}: 165.6 (**C**OO), 153.0, 148.8 (N=**C**-N), 145.6, 141.8, 138.7, 135.5, 130.1, 128.3, 123.2, 122.4, 122.2, 121.5, 119.5, 118.7, 114.5, 111.0, 108.7, 63.3 (**C**H_2O-Ar), 63.1 (**C**H_2OOC-Ar), 42.6 (N-**C**H_2). Selected IR (KBr, cm^{-1}): 3524.5, 3424.5 (ν_{OH}), 2920.7(ν_{CH2}), 1717.7 ($\nu_{C=O}$), 1612.6 ($\nu_{C=N}$), 1593.9, 1585.7, 1520.8, 1485.9, 1474.7, 1463.7 ($\nu_{C=C,\ Ar}$), 1449.7 (δ_{CH2}), 1336.9 ($\nu_{C\text{-}N}$), 1373.1, 1336.7 ($\nu_{C\text{-}N}$), 1243.6 (δ_{OH}), 1205.5 ($\nu_{Ar\text{-}O\text{-}C}$), 1084.2, 1060.3 ($\nu_{Ar\text{-}Cl}$), 1039.7, 1008.2 ($\nu_{Ar\text{-}O\text{-}C}$), 894.9, 879.6, 764.7, 753.1, 743.0 ($\delta_{Ar\text{-}H}$).

8f: white solid. Yield: 82.3%. m. p. 213.9-214.3 °C. Anal. calcd. (%) for $C_{23}H_{19}N_2O_6Cl$: C, 60.73; H, 4.21; N, 6.16. Found (%): C, 60.71; H, 4.13; N, 6.17. MS (ESI, *m/z*), calcd. for $C_{23}H_{19}N_2O_6Cl$: 454.86; found: 455.01 ($M+H^+$). ^{1}H-NMR (600 MHz, DMSO-d_6), δ_{ppm}: 9.28 (s, 2H, Ar-OH), 9.03 (s, 1H, Ar-OH), 7.69-7.65 (q, 2H, Ar-H), 7.35 (d, 2H, Ar-H), 7.29 (t, 1H, Ar-H), 7.23 (t, 1H, Ar-H), 7.11 (d, 2H, Ar-H), 6.87 (s, 2H. Ar-H), 5.45 (s, 2H, CH_2-O-Ar), 4.71 (t, 2H, N-CH_2), 4.56 (t, 2H, CH_2-OOC-Ar). ^{13}C-NMR (150 MHz, DMSO-d_6), δ_{ppm}: 165.6 (**C**OO), 156.5, 149.2 (N=**C**-N), 145.6, 141.8, 138.7, 135.4, 129.3, 125.1, 123.0, 122.1, 119.4, 118.7, 116.6, 110.9, 108.7, 62.9 (**C**H_2O-Ar), 62.8 (**C**H_2OOC-Ar), 42.6 (N-**C**H_2). Selected IR (KBr, cm^{-1}): 3485.7, 3384.1 (ν_{OH}), 2951.0(ν_{CH2}), 1696.4 ($\nu_{C=O}$), 1607.3 ($\nu_{C=N}$), 1530.1, 1490.8, 1468.9 ($\nu_{C=C,\ Ar}$), 1450.0 (δ_{CH2}), 1423.0, 1394.8, 1373.5, 1333.6 ($\nu_{C\text{-}N}$), 1236.7 (δ_{OH}), 1210.2 ($\nu_{Ar\text{-}O\text{-}C}$), 1095.2 ($\nu_{Ar\text{-}Cl}$), 1041.0, 1007.0 ($\nu_{Ar\text{-}O\text{-}C}$), 883.0, 822.1, 766.4, 744.0 ($\delta_{Ar\text{-}H}$).

8g: white solid. Yield: 88.9%. Anal. calcd. (%) for $C_{23}H_{18}N_2O_6Cl_2$: C, 56.46; H, 3.71; N, 5.73. Found (%): C, 56.31; H, 3.54; N, 5.83. MS (ESI, *m/z*), calcd. for $C_{23}H_{18}N_2O_6Cl_2$: 489.30; found: 488.87 (M^+), 490.84 ($M+H^+$). ^{1}H-NMR (400 MHz, DMSO-d_6), δ_{ppm}: 9.21 (s, broad, 3H, Ar-OH), 7.71-7.65 (q, 2H, Ar-H), 7.60 (d, 1H, Ar-H), 7.43-7.38 (m, 2H, Ar-H), 7.30 (t, 1H, Ar-H), 7.24 (t, 1H, Ar-H), 6.86 (s, 2H, Ar-H), 5.57 (s, 2H, CH_2-O-Ar), 4.76 (t, 2H, N-CH_2), 4.57 (t, 2H, CH_2-OOC-Ar). ^{13}C-NMR (100 MHz, DMSO-d_6), δ_{ppm}: 165.6 (**C**OO), 152.1, 148.5 (N=**C**-N), 145.6, 141.7, 138.7, 135.5, 129.4, 128.1, 125.4, 123.2, 122.5, 122.2, 119.5, 118.7, 115.8, 111.0, 108.7, 63.6 (**C**H_2O-Ar), 63.1 (**C**H_2OOC-Ar), 42.6 (N-**C**H_2). Selected IR (KBr, cm^{-1}): 3495.9, 3393.9 (ν_{OH}), 2959.2 (ν_{CH2}), 1712.0 ($\nu_{C=O}$), 1611.9 ($\nu_{C=N}$), 1591.8, 1533.7, 1524.5, 1484.3, 1471.6 ($\nu_{C=C,\ Ar}$), 1422.6 (δ_{CH2}), 1393.1, 1372.4, 1335.0 ($\nu_{C\text{-}N}$), 1286.5, 1245.0 (δ_{OH}), 1207.8 ($\nu_{Ar\text{-}O\text{-}C}$), 1103.2, 1089.4 ($\nu_{Ar\text{-}Cl}$), 1041.7, 1003.5 ($\nu_{Ar\text{-}O\text{-}C}$), 874.7, 809.9, 780.4, 765.1, 741.9 ($\delta_{Ar\text{-}H}$).

8h: white solid. Yield: 87.1%. m. p. 232.3-232.6 °C. Anal. calcd. (%) for $C_{23}H_{19}N_2O_6Br$: C, 55.33; H, 3.84; N, 5.61. Found (%): C, 55.31; H, 3.82; N, 5.65. MS (ESI, *m/z*), calcd. for $C_{23}H_{19}N_2O_6Br$: 499.31; found: 498.96 (M^+), 500.96 ($M+H^+$). ^{1}H-NMR (600 MHz, DMSO-d_6), δ_{ppm}: 9.28 (s, 2H, Ar-OH), 9.03 (s, 1H, Ar-OH), 7.69-7.65 (q, 2H, Ar-H), 7.47 (d, 2H, Ar-H), 7.29 (t, 1H, Ar-H), 7.23 (t, 1H, Ar-H), 7.06 (d, 2H, Ar-H), 6.87 (s, 2H, Ar-H), 5.45 (s, 2H, CH_2-O-Ar), 4.71 (t, 2H, N-CH_2), 4.55 (t, 2H, CH_2-OOC-Ar). ^{13}C-NMR (150 MHz, DMSO-d_6), δ_{ppm}: 165.6 (**C**OO), 157.0, 149.2 (N=**C**-N), 145.6, 141.8, 138.7, 135.4, 132.2, 123.0, 122.1, 119.4, 118.7, 117.2, 112.9, 110.9, 108.7, 62.9 (**C**H_2O-Ar), 62.7 (**C**H_2OOC-Ar), 42.6 (N-**C**H_2). Selected IR (KBr, cm^{-1}): 3499.0, 3380.3 (ν_{OH}), 2951.0 (ν_{CH2}), 1698.1 ($\nu_{C=O}$), 1608.0 ($\nu_{C=N}$), 1581.6, 1529.5, 1488.0, 1469.0 ($\nu_{C=C,\ Ar}$), 1444.4 (δ_{CH2}), 1334.6 ($\nu_{C\text{-}N}$), 1318.4, 1236.3 (δ_{OH}), 1212.2 ($\nu_{Ar\text{-}O\text{-}C}$), 1093.2, 1073.7($\nu_{Ar\text{-}Br}$), 1042.0, 1004.6 ($\nu_{Ar\text{-}O\text{-}C}$), 883.5, 821.9, 804.1, 766.2, 749.3 ($\delta_{Ar\text{-}H}$).

Evaluation on the antimicrobial activities of **8**: The inhibition zone method with filter paper [7] was used to determine the inhibitory effects of the synthesized gallates **8** against pathogenic microorganisms containing *Escherichia coli*, *Staphylococcus aureus*, *Viscous red round yeast*, *Aspergillus niger* and *Penicillium citrinum*, which were all isolated from mildewed leather [7]. The filter-paper discs with diameters of 25 mm were cut, sterilized and soaked for 24 hours in 20 mL dimethyl sulfoxide (DMSO) solution containing 4 mmol of **8**. The obtained discs were air dried, and then put on plate media inoculated with the test microbial suspensions. The test microbial concentrations are 5-10 × 10^5 cfu/mL for bacteria/yeast and 5-10 × 10^4 cfu/mL for moulds. Nutrient agar was used as the

culture media for bacteria, while moulds and yeast were incubated by the rose bengal media. The obtained plate media were put into an incubator of 37 ºC for 24 hours (for bacteria), or 28 ºC for 48 hours (for moulds and yeast), then, the diameters of inhibition zones were measured by a vernier caliper. The discs soaked by pure DMSO were used as controls, and all experiments were conducted in duplicate and the results were confirmed in three independent experiments.

Synthesis of Cr(III) complex of **8h**: 0.4 g of chromium nitrate ($Cr(NO_3)_3 \cdot 9H_2O$) was dissolved in 50 mL of ethanol/water (9 : 1, v/v) mixed solvent, and the prepared solution was added quickly into 50 mL of ethanol/water (9 : 1, v/v) mixed solution containing 0.5 g of 1-ethyl gallate-2-(para-bromo) phenoxymethyl benzimidazole **8h**. The obtained mixture was stirred at r. t. for 3 hours, and then the formed light-green Cr $(OH)_3$ precipitate was remove by the suction filtration, and the filtrate was adjusted to pH 4.0-4.1 with diluted nitric acid solution, and vacuumed to remove most of ethanol solvent. The obtained suspension (10 mL or so) was cooled, filtered, washed with distilled water (3 × 10 mL), and dried to get the Cr(III) complex of **8h** as a yellowish-brown solid. Yield: 0.87 g. m. p. 196.6-197.3 ºC. Anal. calcd. (%) for $C_{46}H_{48}N_5O_{22}Br_2Cr$: C, 44.75; H, 3.92; N, 5.67. Found (%): C, 46.14; H, 4.39; N, 6.02. ^{1}H-NMR (600 MHz, DMSO-d_6), δ_{ppm}: 8.04 (d, 1H, Ar-H), 7.82 (d, 1H, Ar-H), 7.60-7.54 (m, 4H, Ar-H), 7.13 (d, 2H, Ar-H), 6.85 (s, 2H, Ar-H), 5.73 (s, 2H, CH_2-O-Ar), 4.93 (t, 2H, N-CH_2), 4.63 (t, 2H, CH_2-OOC-Ar). ^{13}C-NMR (150 MHz, DMSO-d_6), δ_{ppm}: 165.6 (**C**OO), 156.4, 149.5 (N=**C**-N), 145.6, 138.8, 133.1, 132.4, 125.8, 125.8, 118.6, 117.3, 115.5, 113.8, 113.0, 108.7, 62.4 (**C**H_2O-Ar), 61.4 (**C**H_2OOC-Ar), 44.0 (N-**C**H_2). Selected IR (KBr, cm^{-1}): 3517.2, 3393.9, 3195.9 (ν_{OH}), 1709.1($\nu_{N=O}$), 1673.8 ($\nu_{C=O}$), 1615.5 ($\nu_{C=N}$), 1585.7, 1529.6, 1489.0, 1463.3 ($\nu_{C=C,\ Ar}$), 1447.6 (δ_{CH2}), 1384.2 (ν_{NO3-}), 1357.1(ν_{C-N}), 1239.8 (δ_{OH}), 1230.6 (ν_{Ar-O-C}), 1181.6, 1147.8, 1040.9, 1095. 7, 1068.3 (ν_{Ar-Br}), 1040.9, 1007.1 (ν_{Ar-O-C}), 872.6, 826.5 (δ_{Ar-H}), 815.8 (ν_{NO3-}), 804.1, 770.1, 748.7 (δ_{Ar-H}), 639.0 (ν_{Cr-O}).

Results and Discussion

Synthesis and structure analysis for compounds **8**

As shown in Scheme 1, an indirect esterification protocol [7] was adopted to synthesize the target gallates containing the benzimidazole moiety. The gallic acid was used as starting material, and its three phenolic hydroxyl groups was firstly protected by the reaction with acetic anhydride in the presence of concentrated sulfuric acid (H_2SO_4) at 90 ºC. Then, the obtained trisacetyl gallic acid (**2**) was refluxed for 3 hours in thionyl chloride ($SOCl_2$) with the aid of dimethyl formamide (DMF) to prepare the trisacetyl galloyl chloride (**3**) that can efficiently react with 2-substituted phenoxymethyl benzimidazoles (**6**)[49,50] in the presence of triethylamine as the acid binding agent. Finally, the protective acetyl groups of the key intermediate (**7**) were eliminated by adding hydrazine hydrate to get the final 1-ethyl gallate-2-substituted phenoxymethyl benzimidazoles (**8**). This route resulted in high yield up to 91%. All the obtained gallates are white solids and exhibit good solubility in common organic solvents such as CH_2Cl_2, chloroform ($CHCl_3$), tetrahydrofuran (THF), methanol, ethanol, acetone, acetonitrile, DMF and DMSO.

Elemental analysis, MS, ^{1}H, ^{13}C-NMR and IR techniques were used to characterize the molecular structures of the compounds **8**. Similar ^{1}H and ^{13}C-NMR spectra in DMSO-d_6 were observed for all the obtained gallates. For example, in the ^{1}H-NMR spectrum of 1-ethyl gallate-2-bromine phenoxymethyl benzimidazoles (**8h**), the two single peaks at 9.28 and 9.03 ppm can be asigned to the three protons of its contiguous phenolic hydroxyls, and the single peak at 5.45 ppm corresponded to the two protons of methoxy group, while the ethyl protons were found at 4.71 ppm and 4.55ppm and both of them are triplet peaks. In the ^{13}C-NMR spectrum of **8h**, carbonyl carbon was observed at 165.6 ppm and methoxy carbon was located at 62.9 ppm, while the peaks at 62.7 and 42.6 ppm are assigned to the two ethyl carbons. Notably, the type and location of substituent groups on the phenoxymethyl units can result in moderate effect on the position of these charcteristic peaks. All the other peaks of the ^{1}H and ^{13}C-NMR are well assigned and match well with the structures of the target compounds **8**.

All the target compounds showed similar FT-IR spectra. The stretching vibration of phenolic hydroxyl groups (Ar-OH) were observed at 3400-3500 cm^{-1} or so as broad absorption bands. The strong peaks at 1700 cm^{-1} or so corresponded to the stretching vibration of ester C=O groups, while the peaks assigned to the stretching vibration of C=N groups of benzimidazole rings were found at 1620 cm^{-1} nearby. The absorption bands found in the range of 1333-1347 cm^{-1} were attributed to the C-N bond, and the peaks due to the presence of ether bond

(Ar-O-C) were found at 1225-1244 cm^{-1}. The substituent groups in the phenoxymethyl structures also exhibit obvious effect on the position of these peaks. Furthermore, the several absorption peaks at 1600-1450 cm^{-1} were the characteristic skeletal vibration of benzene rings.

For compound **8h**, Single crystal suitable for the X-ray diffraction analysis was obtained by slow evaporation of its hydrous ethanol solution. Crystal data and structure refinements are given in Table-1, while Fig. 1 clearly shows the crystal molecular structure. Selected bond lengths and angles are listed in Table-2, and hydrogen bond lengths bond and angles were given in Table-3.

Single crystal X-ray analysis further confirmed the success of the esterification reaction between the gallic acid and 1-hydroxyethyl 2-substituted phenoxymethyl benzimidazole. As shown in Fig. 1, the carbonyl carbon (C17) is connected to the hydroxyl oxygen (O2) to form the ester bond. Notably, the three moieties of compound **8h**, namely, benzimidazole, substituted phenoxymethyl and gallate units, are not co-plane, and the formed intersection angles between these three planes are 59.23°, 75.56° and 19.60°, respectively. The bond lengths of C16-O2, C17-O2 and C17-O3 are 1.445(3) Å, 1.334(3) Å and 1.208(3) Å, respectively, while the bond angles of C17-O2-C16, O3-C17-O2 and O2-C17-C18 are 116.1(2)°, 122.2(3)° and 113.4(2)°, respectively.

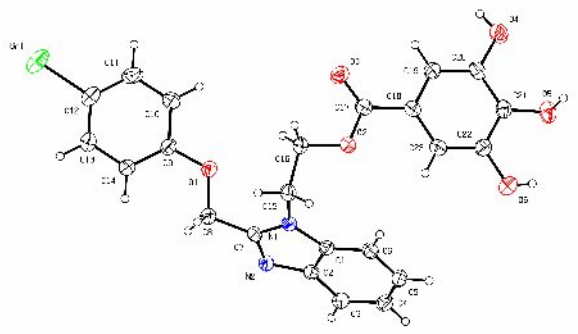

Fig. 1: Crystal molecular structure of **8h**.

Furthermore, many intramolecular and intermolecular hydrogen bonds were observed in the unit cell of **8h**. Specifically, there exists an intramolecular oxy-hydrogen linkage (O6-H6...O5) between hydroxyl oxygen (O5) and adjacent hydrogen (H6) with bond length of 2.273 Å and bond angle of 113.55°, while another oxy-hydrogen linkage (C16-H16A ...O1) was found between ether oxygen (O1) atom and the methylene hydrogen (H16A) of ester group, and its bond length is 2.566 Å and bond angle is 128.72°. Five intermolecular hydrogen bonds, namely oxy-hydrogen linkages of C6-H6 ...$O6^1$, C15-H15B .$O5^2$, C19-H19 ...$O3^3$ and O4-H4...$O3^4$, and nitrogen-hydrogen linkage of O5-H5...$N2^5$ were also observed, their bond lengths are successively 2.563 Å, 2.604 Å, 2.556 Å, 2.047 Å and 1.875 Å, and their bond angles are 160.86°, 139.70°, 132.68°, 168.61° and 176.21°, respectively.

Table-1: Crystal data and structure refinement details for **8h**.

Formula	$C_{23}H_{19}BrN_2O_6$	Formula weight	499.31
Temperature/K	293.15	Crystal system	monoclinic
Space group, F(000)	$P2_1/n$, 1016.0	$\rho_{calc}mg/mm^3$, μ/mm^{-1}	1.594, 2.021,
a/Å, b/Å, c/Å	11.6438(8), 12.6705(5), 15.0164(8)	Crystal size/mm^3	0.4 × 0.4 × 0.25
α/°, β/°, γ/°	90, 110.136(7), 90	Volume/$Å^3$, Z	2080.0(2), 4
Radiation	MoKα (λ = 0.71073 Å)	2θ range for data collection	5.78 to 52.746°
Index ranges	$-13 \le h \le 14$, $-15 \le k \le 15$, $-17 \le l \le 18$	Reflections collected	9123
Independent reflections	4250[R_{int}= 0.0238, R_{sigma}= 0.0464]	Data/restraints/parameters	4250/0/292
Final R indexes [all data]	R_1=0.0835, wR_2=0.0946	Goodness-of-fit on F^2	1.004
Final R indexes [I ≥2σ (I)]	R_1=0.0434, wR_2=0.0805	Largest diff. peak/hole/e$Å^{-3}$	0.38/-0.55

Table-2: Selected bond lengths (Å) and angles (°) for **8h**.

Bond	Length (Å)	Bond	Length (Å)	Bond	Length (Å)
Br 1-C12	1.897(3)	C16-O2	1.445(3)	C17-O2	1.334(3)
C17-O3	1.208(3)	C17-C18	1.481(4)	C7-N1	1.358(3)
C7-N2	1.324(3)	C15-N1	1.457(3)	C1-N1	1.391(3)
C2-N2	1.387(3)	C20-O4	1.376(3)	C21-O5	1.365(3)
C22-O6	1.369(3)	C9-O1	1.374(3)	C8-O1	1.423(3)
Angle	(°)	Angle	(°)	Angle	(°)
C11-C12-*Br* 1	119.4(2)	C13-C12-*Br* 1	120.4(2)	O3-C17-O2	122.2(3)
O3-C17-C18	124.3(3)	O2-C16-C15	107.6(2)	C17-O2-C16	116.1(2)
O2-C17-C18	113.4(2)	N1-C15-C16	113.0(2)		

Table-3: Hydrogen bond lengths (Å) and bond angles (°) for **8h**.

D - H ... A	D-H(Å)	H…A(Å)	D…A(Å)	<(DHA)(°)
C6-H6 ...O6[1]	0.930	2.563	3.455	160.86
C15-H15B ...O5[2]	0.970	2.604	3.402	139.70
C16-H16A ...O1	0.970	2.566	3.262	128.72
C19-H19 ...O3[3]	0.930	2.556	3.259	132.68
O4-H4...O3[4]	0.820	2.047	2.856	168.61
O5-H5...N2[5]	0.820	1.875	2.694	176.21
O6-H6...O5	0.820	2.273	2.707	113.55

Symmetry code: [1][-x, -y+1, -z+1], [2][x+1/2, -y+3/2, z-1/2], [3][-x, -y+2, -z+1], [4][-x, -y+2, -z+1], [5][x-1, y, z]

Antimicrobial Activities of Compounds **8**

Table-4: Diameters of inhibitory zones of compounds **8** against tested microorganisms (mm).

Compounds	*Escherichia coli*	*Staphylococcus aureus*	*Viscous red round yeast*	*Aspergillus niger*	*Penicillium citrinum*
Control	25.00	25.00	25.00	25.00	25.00
8a	26.62	26.85	26.36	25.94	25.80
8b	26.81	27.03	26.02	26.42	26.52
8c	27.02	28.48	28.48	26.34	26.68
8d	27.13	26.90	27.03	26.36	26.38
8e	27.68	27.77	27.66	26.13	25.76
8f	28.74	28.62	27.58	26.22	26.26
8g	27.73	28.40	27.92	26.14	25.96
8h	28.70	29.86	29.95	26.74	26.88

As shown in Table-4, the prepared eight target compounds **8** exhibited varied inhibitory effects against tested bacteria, yeast and moulds, and especially, **8h**, 1-ethyl gallate-2-(para-bromo) phenoxymethyl benzimidazole, shows the greatest antimicrobial activity. In general, the diameters of inhibition zones against Gram negative *Escherichia coli*, Gram positive *Staphylococcus aureus* and *Viscous red round yeast* are bigger than that against *Aspergillus niger* and *Penicillium citrinum*.

Moreover, the type and position of substituent groups distinctly influence the antimicrobial activities of 1-ethyl gallate-2-substituted phenoxymethyl benzimidazoles. For instance, **8d**, **8f**, and **8h**, which have para-substituted CH_3, Cl and Br groups, respectively, revealed successively increased diameters of inhibitory zones of 26.90, 28.62 and 29.86 mm against the Gram positive *Staphylococcus aureus*. Similar tendency was also observed for the tested yeast and moulds. These results indicate that electron-donating CH_3 group is adverse for the improvement of antibacterial effects of these gallates; on the contrary, electron-drawing groups such as Cl and Br groups can enhance their antibacterial properties. Furthermore, the stronger the electrical absorption is, the better the antimicrobial effect is. For the compounds **8b**, **8c** and **8d**, which contain the electron-donating CH_3 group at ortho-, meta- and para-postions, respectively, the inhibition zones of **8c** and **8d** are always bigger than that of **8b**. Similarly, for **8e** and **8f**, which contain electron-drawing Cl group at ortho- and para-postions, respectively, the bigger inhibition zones were invariably observed for the latter. These data confirm that meta- and para-substitution can improve the antimicrobial activities of the target compounds.

Molecular structure of Cr(III) complex of **8h**

The obtained Cr(III) complex of **8h** was well characterized by many techniques containing IR, NMR, UV-vis, TG and elemental analysis to realize its molecular structure. The melt point of the obtained product, 196.6-197.3 °C, is distinctly lower than that (232.3-232.6 °C) of the starting compound **8h**, which indicates the successful synthesis of chromium complex. The comparison of FI-IR spectra (Fig. 2) can further confirmed this point. Obvious changes were observed for the stretching vibration peaks assigned to the phenolic hydroxyl groups. Specifically, the peaks at 3499.0 and 3380.3 cm^{-1} of ligand **8h** disappeared, which shows that the hydroxyl groups take part in the coordination with Cr(III) atom [54-57]. The new peaks at 3517.2, 3393.9 and 3195.9 cm^{-1} can be attributed to the stretching vibration of water O-H and residual phenolic O-H.[58, 59] The stretching vibration peak of C=O group shifted from 1698.1 cm^{-1} in **8h** to 1673.8 cm^{-1} in the complex, while the two stretching vibration peaks corresponding the ester bond (C-O-C) were observed at 1318.4 and 1212.2 cm^{-1} for the ligand, 1357.1 and 1230.6 cm^{-1} for the complex, respectively. The difference values (Δν) are 106 and 127 cm^{-1}, respectively, and both of them are less than 200 cm^{-1}, which confirmed that ester oxygen atoms did not coordinate with meal atom.[54,59,60] The shifts of these peaks are caused by the change of corresponding electron cloud density[61-63] because of the formation of Cr(III) complex, and similar shift was also found for the peaks assigned to the C=N bond of benzimidazole ring, C=C bonds in benzene rings and C-Br bond. The strong peak at 1239.8 cm^{-1} was attributed to the flexural vibration of O-H group [54, 58], which further indicates the presence of uncoordinated O-H group, while the signal at 639.0 cm^{-1} corrsponding to the Cr-O bond [58, 61] proved the coordinative atom is oxygen of phenolic O-H groups. Furthermore, the new peak at 1709.1 cm^{-1} can be assigned to $\nu_{C=O}$ of nitrate, while the peak at 1384.2 cm^{-1} is also the characteistic peak of the inoganic anion. These results verify the presence of nitrate group in the molecular structue of the chromium complex.

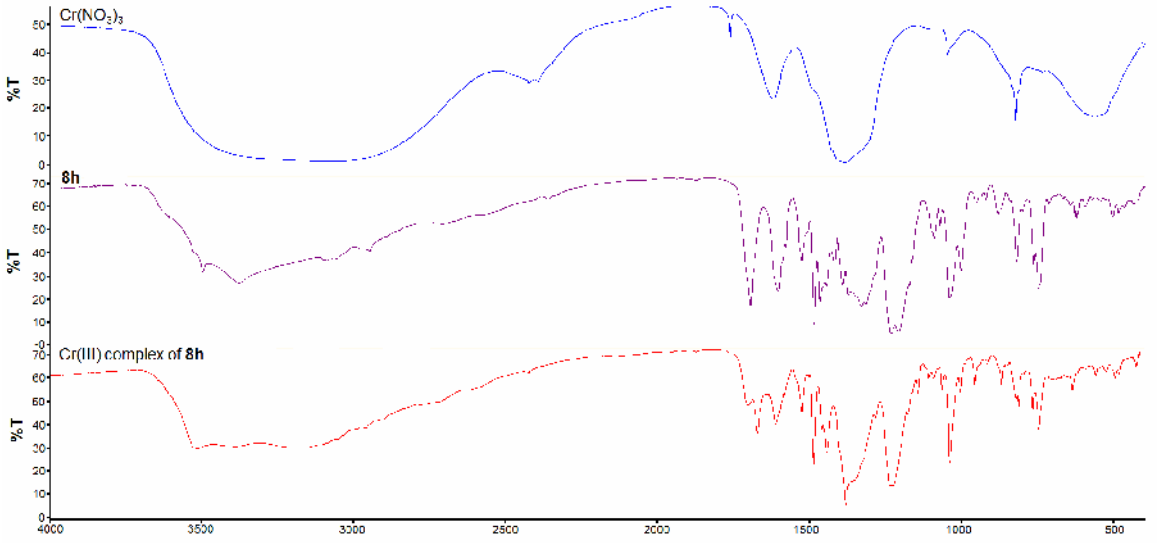

Fig. 2: FI-IR spectra of $Cr(NO_3)_3$, **8h** and its Cr(III) complex.

^{1}H and ^{13}C-NMR spectra of the complex were checked in DMSO-d_6 as shown in Fig. S36 and S37. As expected, the peaks close to 9.0 ppm, corresponding to the protons of O-H groups, were not observed in the ^{1}H-NMR spectrum of the complex, which further confirms that the O-H groups were coordinated with Cr(III) atom. The other peaks of the ^{1}H-NMR spectrum were well assigned and matched the structure of the ligand **8h**, which indicates the integrity of ligand **8h** was not destroyed during the preparation of Cr(III) complex. However, obvious shifts were observed for all these peaks due to the interaction between the chromium atom and ligand. Moreover, the peaks of ^{13}C-NMR spectrum were also well assigned and illustrated the integrity of ligand.

As shown in Fig. 3, the UV-vis spectra of Cr(III) complex, ligand **8h** and $Cr(NO_3)_3$ are compared in ethanol/water. The UV-vis spectrum of the complex shows a strong absorption band at 301 nm, whereas the λ_{max} of the ligand **8h** and $Cr(NO_3)_3$ are 300 and 299 nm, respectively. This absorption at 301 nm corresponds to the π-π* transition that is known for both substituted benzene and NO_3 units. The peak corresponding to the d-d* transition of NO_3 group was observed in the complex as two shoulders at 350 and 400 nm, respectively, which shows the existence of NO_3 unit in the molecular structure of the complex.

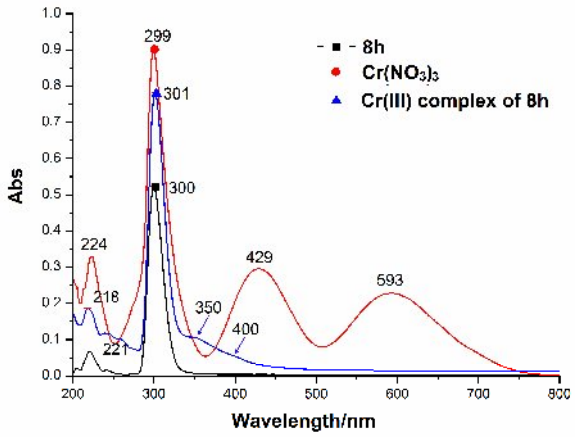

Fig. 3: UV-Vis spectra of $Cr(NO_3)_3$, 8h and its Cr(III) complex in ethanol/water (9:1, v/v).

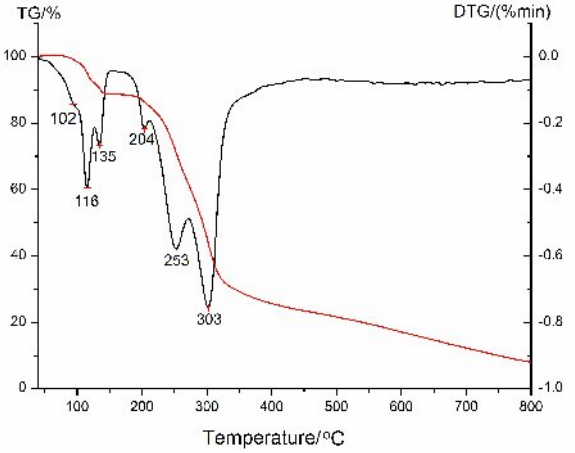

Fig. 4: TG and DTG curves of Cr(III) complex of **8h.**

The TG and DTG curves of the Cr(III) complex were drawn in the range of 40-800 ^{o}C, and six obvious weight-loss bands were observed (Fig. 4). The first weight-loss band was found at 100-106 ^{o}C with the weight-loss ratio of 4% or so, and probably caused by the loss of free water. In the range of 106-127 ^{o}C, another about 4% weight is decreased, and it can be assigned the loss of hydrogen-binding water in the complex. The weight-loss at 127-152 ^{o}C is also 4% and resulted from the split of NO_3 units, while the 3% weight loss at 152-211 ^{o}C is a sign of losing water coordinating with chromium atom. The last two weight-loss bands, 211-271 ^{o}C and 271-341 ^{o}C, resepctivley, can be attributed to the loss of two ligand units. Finally, residual 8% weight is retained.

Also, elemental analysis provided helpful information for the structural deduction of the Cr(III) complex. As shown in Fig 5, a possible molecular structure for the Cr(III) complex of **8h** was drawn according to the data analysis for the above various tests. The molecular formula is $C_{46}H_{48}N_5O_{22}Br_2Cr$, and the calculated molecular weight is 1234.70. The contens of C, H and N are 44.75%, 3.92% and 5.67%, respectively, and these vaules are very close to the found results of 46.14%, 4.39% and 6.02%. The errors may be caused by the little residual ethanol whose presence was confirmed by the small peaks in the ^{1}H-NMR spectrum of the complex. The sturcrtue in Fig. 5 can adequately explain the weight-loss features in Fig. 4, and the calculated residual weight is 6.2% as Cr_2O_3 [54] that is close to the observed 8% or so. Furthermore, the hydrogen bonds between the uncoordinated hydroxy group and water probably resulted in the lack of detection for these O-H protons in the ^{1}H-NMR spectrum of the complex.

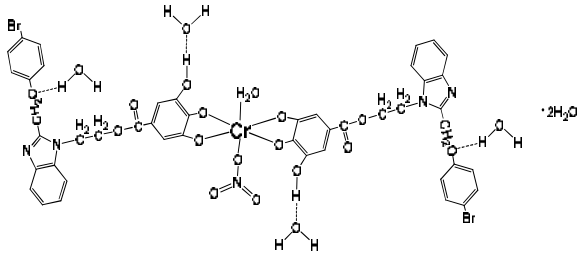

Fig. 5: The possible molecular structure for the Cr(III) complex of **8h**.

Conclusion

Following the successive N-hydroxyethylation and indirect esterification reactions, the active structure of gallic acid ester was successfully attached to the N (or 1) positon of benzimidazole to get eight target compounds of 1-ethyl gallate-2-substituted phenoxymethyl benzimidazoles. The antimicrobial activities of these compounds can be regulated by changing the substituent groups in the phenoxymethyl portion, and specifically, the electron-drawing groups such as Cl and Br at meta- or para-postions can improve their antimicrobial activities, while substituent groups with electron-donating property at ortho-position will exhibit the opposite effect. Moreover, a target compound **8h** can be used as a ligand to coordinate with Cr(III) salt, and in the obtained complex, adjacent hydroxyl groups of two **8h** molecules, nitrate and H_2O take part in the direct coordination with Cr(III) atom.

Supplementary material

Crystallographic data for the compound **8h** has been deposited in the Cambridge Crystallographic Data Centre with the deposition number of CCDC 1482283. These data can be obtained free of charge via http://www.ccdc.cam.ac.uk/data request/cif, by e-mailing data request@ccdc.cam.ac.uk or by contacting the Cambridge Crystallographic Data Centre, 12, Union Road, Cambridge CB2 1EZ, UK; fax: +44-1223-336033.

Acknowledgements

The project is financially supported by the National Science Foundation of China (No. 21106088) and the Ph. D. Programs Foundation of Ministry of Education of China (No. 20110181120079).

References

1. S. Choubey, L. R. Varughese, V. Kumar and V. Beniwal, Medicinal Importance of Gallic Acid and its Ester Derivatives: a Patent Review, *Pharm Pat Anal.*, **4**, 305 (2015).
2. C. Locatelli, F. B. Filippin-Monteiro and T. B. Creczynski-Pasa, Alkyl Esters of Gallic Acid as Anticancer Agents: A review, *Eur. J. Med. Chem.*, **60**, 233 (2013).
3. J. Steinmann, J. Buer, T. Pietschmann and E. Steinmann, Anti-Infective Properties of Epigallocatechin-3-gallate (EGCG), a Component of Green Tea, *Br. J. Pharmacol.*, **168**, 1059 (2013).
4. A. Chowdhury, J. Sarkar, T. Chakraborti, P. K. Pramanik and S. Chakraborti, Protective Role of Epigallocatechin-3-gallate in Health and

Disease: A Perspective, *Biomed. Pharmacother*, **78**, 50 (2016).

5. E. Rivero Buceta, P. Carrero, E. G. Doyagueez, A. Madrona, E. Quesada, M. J. Camarasa, M. J. Perez-Perez, P. Leyssen, J. Paeshuyse, J. Balzarini, J. Neyts and A. San-Félix, Linear and Branched Alkyl-Esters and Amides of Gallic Acid and other (mono-, di- and tri-) Hydroxy Benzoyl Derivatives as Promising Anti-HCV Inhibitors, *Eur. J. Med. Chem.*, **92**, 656 (2015).
6. Y. Matsumoto, K. Kaihatsu, K. Nishino, M. Ogawa, N. Kato and A. Yamaguchi, Antibacterial and Antifungal Activities of New Acylated Derivatives of *Epigallocatechin gallate*, *Front. Microbiol.*, **3**, 53 (2012).
7. Z. Y. Wang, H. B. Gu and W. Y. Chen. Synthesis, Characterization and Antimicrobial Activity of Three Gallates Containing Imidazole, Benzimidazole and Triclosan Units, *Asian J. Chem.*, **26**, 513 (2014).
8. Kubo, P. Xiao and K. Fujita, Antifungal Activity of Octyl Gallate: Structural Criteria and Mode of Action, *Bioorg. Med. Chem. Lett.*, **11**, 347 (2001).
9. A. Guida, A. Lucchese, G. Minervini, V. De Gregorio, L. Coretti, E. Grimaldi, D. Minervini, R. Serpico and G. Donnarumma, In-Vitro Analysis of Antifungal Activity of Epigallocatechin-Gallate: Preliminary Study, *Eur. J. Inflamm.*, **11**, 911 (2013).
10. H. J. Jung and C. J. Lim, The Antiangiogenic and Antinociceptive Activities of *n*-Propyl Gallate, *Phytother. Res.*, **25**, 1570 (2011).
11. H. S. Kim, M. J. Quon and J. A Kim, New Insights into the Mechanisms of Polyphenols Beyond Antioxidant Properties; Lessons from the Green Tea Polyphenol, Epigallocatechin 3-Gallate, *Redox Biology*, **2**, 187 (2014).
12. N. M. A. El-Ebiary, R. H. Swellem, A. T. H. Mossa and G. A. M. Nawwar, Synthesis and Antioxidant Activity of New Pyridines Containing Gallate Moieties, *Arch. Pharm.*, **343**, 528 (2010).
13. C. Y. Shen, L. L. Chen, L. B. Jiang and T. Y. Y. Lai, Neuroprotective Effect of epigallocatechin-3-gallate in a Mouse Model of Chronic Glaucoma, *Neurosci. Lett.*, **600,** 132 (2015).
14. B. N. Singh, S. Shankar and R. K. Srivastava, Green Tea Catechin, epigallocatechin-3-gallate (EGCG): Mechanisms, Perspectives and Clinical Applications, *Biochem. Pharmacol.* **82**, 1807 (2011).
15. H. B. Gu, W. Y. Chen, C. Q. Zhao and X. Hao. New Antimicrobial Complex of Copper(II) with Benzothizole Derivative: Synthesis and Application in Leather Industry, *J. Am. Leather Chem. Assoc.*, **103**, 114 (2008).
16. D. Seenaiah, P. R. Reddy, G. M. Reddy, A. Padmaja, V. Padmavathi and N. S. Krishna, Synthesis, Antimicrobial and Cytotoxic Activities of Pyrimidinyl Benzoxazole, Benzothiazole and Benzimidazole, *Eur. J. Med. Chem.*, **77**, 1 (2014).
17. U. Kalinowska-Lis, E. M. Szewczyk, L. Checinska, J. M. Wojciechowski, W. M. Wolf and J. Ochocki, Synthesis, Characterization, and Antimicrobial Activity of silver(I) and copper(II) Complexes of Phosphate Derivatives of Pyridine and Benzimidazole, *ChemMedChem*, **9**, 169 (2014).
18. C. Desai, D. D. Pandya, K. A. Bhatt, G. M. Kotadiya and P. Desai, Synthesis, Antimicrobial, and Cytotoxic Activities of Novel Benzimidazole Derivatives Bearing Cyanopyridine and 4-thiazolidinone Motifs, *Med. Chem. Res.*, **23**, 3823 (2014).
19. D. Song, S. Ma, Recent Development of Benzimidazole-Containing Antibacterial Agents, *ChemMedChem*, **11**, 646 (2016).
20. R. S. Keri, A. Hiremathad, S. Budagumpi and B. M. Nagaraja, Comprehensive Review in Current Developments of Benzimidazole-Based Medicinal Chemistry, *Chem. Biol. Drug Des.*, **86**, 799 (2015).
21. G. J. Kumar, S. N. Kumar, D. Thummuri, L. B. S. Adari, V. G. M. Naidu, K. Srinivas and V. J. Rao, Synthesis and Characterization of New *s*-triazine bearing Benzimidazole and Benzothiazole Derivatives as Anticancer Agents, *Med. Chem. Res.*, **24**, 3991 (2015).
22. T. Wu, Z. Jiang, J. J. Shen, H. Yi, Y. C. Zhan, M. Q. Sha, Z. Wang, S. T. Xue, Z and R. Li, Design, Synthesis and Biological Evaluation of Novel Benzimidazole-2-substituted phenyl or Pyridine Propyl Ketene Derivatives as Antitumour Agents, *Eur. J. Med. Chem.*, **114**, 328 (2016).
23. B. Narasimhan, D. Sharma and P. Kumar, Benzimidazole: a Medicinally Important Heterocyclic Moiety, *Med. Chem. Res.*, **21**, 269 (2012).
24. J. Perez Villanueva, R. Santos, A. Hernandez-Campos, M. A. Giulianotti, R.

Castillo and J. L. Medina-Franco, Structure-Activity Relationships of Benzimidazole Derivatives as Antiparasitic Agents: Dual Activity-Difference (DAD) Maps, *MedChemComm*, **2**, 44 (2011).

25. Y. C. Zhang, J. Y. Xu, Y. M. Li, H. Q. Yao and X. M. Wu, Design, Synthesis and Pharmacological Evaluation of Novel NO-Releasing Benzimidazolehybrids as Potential Antihypertensive Candidate, *Chem. Biol. Drug Des.*, **85**, 541 (2015).
26. M. Boiani and M. Gonzalez, Imidazole and Benzimidazole Derivatives as Chemotherapeutic Agents, *Mini-Rev. Med. Chem.*, **5**, 409 (2005).
27. J. F. Miller, E. M. Turner, K. S. Gudmundsson, S. Jenkinson, A. Spaltenstein, M. Thomson and P. Wheelan, Novel *N*-substituted benzimidazole CXCR4 Antagonists as Potential Anti-HIV Agents, *Bioorg. Med. Chem. Lett.*, **20**, 2125 (2010).
28. Shah, S. Chhabra, S. K. Shrivastava and P. Mishra, Benzimidazole: a Promising Pharmacophore, *Med. Chem. Res.*, **22**, 5077 (2013).
29. H. Li, D. Z. Kang, S. B. Wang, G. H. Gong and Z. S. Quan, Synthesis and Evaluation of the Anticonvulsant Activity of 9-alkyl-2,9-dihydro-3H-1,2,4-triazolo[4,3-a]benzimidazole-3-one Derivatives, *Lat. Am. J. Pharm.*, **34**, 5 (2015).
30. N. C. Desai, N. R. Shihory, G. M. Kotadiya and P. Desai, Synthesis, Antibacterial and Antitubercular Activities of Benzimidazole Bearing Substituted 2-pyridone Motifs, *Eur. J. Med. Chem.*, **82**, 480 (2014).
31. E. Mentese, F. Yilmaz, N. Baltas, O. Bekircan and B. Kahveci, Synthesis and Antioxidant Activities of Some New Triheterocyclic Compounds Containingbenzimidazole, Thiophene, and 1,2,4-triazole Rings, *J. Enzym. Inhib. Med. Chem.*, **30**, 435 (2015).
32. R. V. Shingalapur, K. M. Hosamani, R. S. Keri and M. H. Hugar, Derivatives of Benzimidazole Pharmacophore: Synthesis, Anticonvulsant, Antidiabetic and DNA Cleavage Studies, *Eur. J. Med. Chem.*, **45**, 1753 (2010).
33. A. Kamil, S. Akhter, M. Ahmed, G. H. Rizwani, S. Hassan, S. Naeem, S. Jahan, R. Khursheed and H. Zahid, Antimalarial and Insecticidal Activities of Newly Synthesized Derivatives of Benzimidazole, *Pak. J. Pharm. Sci.*, **28**, 2179 (2015).
34. Z. Y. Wang, H. B. Gu, J. C. Wu and W. Y. Chen. Synthesis and Structural Characterization of 2-(hydroxyethoxy substituted) phenyl benzimidazoles, *Asian J. Chem.*, **27**, 1719 (2015).
35. X. K. Zhu, Y. J. Yang, Y. Zhong and K. H. Luo, Study on the Synthesis and Antimicrobial Activity of Substituted Phenoxy Acetic Acids, *J. Southwest Univ. (Nat. Sci. Ed.)*, **29**, 126 (2007).
36. H. B. Gu, L. Wang, C. Q. Zhao, Y. Gong and W. Y. Chen. Synthesis, Crystal Structure and Antimicrobial Activity of a New Ternary Copper(II) Complex with Para-Formyl Phenoxyacetic Acid and 2-Amino Benzothiazole, *Chin. J. Inorg. Chem.*, **25**, 1464 (2009).
37. H. B. Gu, L. Long, P. P. Li, L. Wang and W. Y. Chen. Synthesis, Crystal Structure and Antimicrobial Activity of a New Ternary Copper(II) Complex with *p*-chlorophenoxyacetic acid and 2-amino benzothiazole, *Chin. J. Struct. Chem.*, **29**, 676 (2010).
38. H. B. Gu, Z. Y. Wang and W. Y. Chen. Ternary zinc (II) complex with 2-amino benzothiazole and phenoxyacetic acid: Synthesis, Crystal Structure and Antimicrobial Activity, *Asian J. Chem.*, **24**, 915 (2012).
39. H. B. Gu, Z. Y. Wang and W. Y. Chen, Copper(II) Complexes Bearing 2-amino Benzothiazole and Phenoxyacetic Acid Derivatives: Coordination Modes and Antimicrobial Activity, *Chin. J. Inorg. Chem.*, **28**, 591 (2012).
40. H. Chen, S. Q. Huang, Y. M. Wen and S. D. Li, Catalytic synthesis of benzimidazolyl-phenoxyacetic acid O-acetyllactosyl saccharide esters by DMAP/Et_3N and Antiviral Activity Against TMV, *J. Chem. Res.*, **10**, 626 (2005).
41. Z. Li, X. K. Wang, X. Xu, J. Y. Yang, W. T. Xia, X. H. Zhou, W. L. Huang and H. Qian, Design, Synthesis and Biological Activity of Phenoxyacetic Acid Derivatives as Novel Free Fatty Acid Receptor 1 agonists, *Bioorg. Med. Chem.*, **23**, 7158 (2015).
42. X. K. Wang, T. X. Zhao, B. W. Yang, Z. Li, J. Cui, Y. X. Dai, Q. Q., Qiu, H. Qiang, W. L. Huang and H. Qian, Synthesis and Biological Evaluation of Phenoxyacetic Acid Derivatives as Novel Free Fatty Acid Receptor 1 Agonists, *Bioorg. Med. Chem.*, **23**, 132 (2015).
43. A. K. Jain, V. Ravichandran, R. Singh, V. Mourya and R. K. Agrawal, QSAR Study of 2,4-disubstituted Phenoxyacetic Acid Derivatives as a CRTh2 Receptor Antagonists, *Chem. Pap.*, **63**, 464 (2009).
44. H. Arakawa, N. Watanabe and H. A. Tajmir-Riahi, Calf-Thymus DNA Interaction

with Cr(III)-Gallate and Cr(III)-Ethyl Gallate Studied by FTIR Spectroscopy and Capillary Electrophoresis, *Bull. Chem. Soc. Jpn.*, **74**, 1075 (2001).

45. H. Arakawa and M. S. Tang, Recognition and Incision of Cr(III) Ligand-Conjugated DNA Adducts by the Nucleotide Excision Repair Proteins UvrABC: Importance of the Cr(III)-Purine Moiety in the Enzymatic Reaction, *Chem. Res. Toxicol.*, **21**, 1284 (2008).
46. M. Y. Moridani, J. Pourahmad, H. Bui, A. Siraki and P. J. O'Brien, Dietary Flavonoid Iron Complexes as Cytoprotective Superoxide Radical Scavengers, *Free Radic. Biol. Med.*, **34**, 243 (2003).
47. M. F. Ullah, S. H. Bhat, E. Husain, F. Abu-Duhier, S. M. Hadi, F. Sarkar and A. Ahmad, Cancer Chemopreventive Pharmacology of Phytochemicals Derived from Plants of Dietary and Non-Dietary Origin: Implication for Alternative and Complementary Approaches, *Phytochem. Rev.*, **13**, 811 (2014).
48. J. Sang, C. B. Zheng, X. H. Qiang, H. Zhang and M. M. Hou, Tanning Ability of Combining Gallic Acid with Chromium-Aluminum, *Chian Leather*, **39**, 17 (2010).
49. J. C. Wu, L. Zhao, C. Q. Zhao, Z. Y. Wang, H. B. Gu and W. Y. Chen, 1-Hydroxyethyl-2-Substituted Phenoxymethyl Benzimidazoles: Synthesis and Crystal Structures, *J. Chem. Soc. Pak.*, **38**, 307 (2016).
50. J. C. Wu, L. Zhao, C. Q. Zhao, Z. Y. Wang, H. B. Gu and W. Y. Chen, Synthesis and Molecular Structures of 1-hydroxyethyl-2-(p-substituted) phenoxymethyl benzimidazoles, *J. Chem. Soc. Pak.*, **38**, 974 (2016).
51. O. V. Dolomanov, L. J. Bourhis, R. J. Gildea, J. A. K. Howard and H. Puschmann, OLEX2: a Complete Structure Solution, Refinement and Analysis Program. *J. Appl. Cryst.*, **42**, 339 (2009).
52. SUPERFLIP, *J. Appl. Cryst.*, **40**, 786 (2007).
53. SHELXL, G. M. Sheldrick, *Acta Cryst.*, **A64**, 112 (2008).
54. M. S. Masoud, S. S. Hagagg, A. E. Ali and E. M. Nasr, Synthesis and Spectroscopic Characterization of Gallic Acid and Some of Its Azo Complexes, *J. Mol. Struct.*, **1014**, 17 (2012).
55. W. L. Hong, J. H. Liu, F. Q. Zhao, Y. M. Li, Z. K. Luo, D. Y. Tian and P. X. Zhang, Synthesis and Combustion Catalytic Activity of Nanoparticle Pb(II)-Gallate Complex, *Acta Chim. Sin.*, **63**, 249 (2005).
56. L. R. Zhang, K. L. Chen, L. Lin, X. Yang and G. L. Zou, Study on the Complexes of Gallic Acid-Zn(II) and the Interaction with DNA, *J. Wuhan Univ. (Nat. Sci. Ed.)*, **50**, 234 (2004).
57. Q. K. Wang, L. M. Zhou, S. P. Pu, J. Peng, Q. Zhang, L. M. Liu, Y. X. Liao and J. Jin, Synthesis, Characterization and Antitumor Activities of *cis*-ammine gallic acid (2-methylpyridine) platinum(II), *Precious Metals*, **34**, 55 (2013).
58. L. Wu, M. Yan, J. G. Wang, Z. W. Guan, Z. L. Xia, X. R. Qin and D. L. Yi, Synthesis, Characterization, and Simulation of SOD of M (M: Fe(III), Cr(III), Cu(II))-Propyl Gallate Complexes, *Chin. J. Applied Chem.*, **27**, 328 (2010).
59. Q. K. Wang, L. M. Zhou, S. P. Pu, J. Peng, Q. Zhang, L. M. Liu, Y. X. Liao and J. Jin, Synthesis, Characterization and Antitumor Activities of *cis*-Ammine Gallic Acid (2-methylpyridine) platinum(II), *Precious Metals*, **34**, 55 (2013).
60. Z. Yang, G. R. Pang, J. P. Li, Molecularly Imprinted Sensor Based on Lead-Gallic Acid Complexes and Its Application, *J. Anal. Sci.*, **31**, 470 (2015).
61. M. Yan, L. Wu, X. R. Qin, R. Liu, D. L. Yi and Z. L. Xia, Study on Synthesis of Complex of Propyl Gallate-Chromium (III), *Chem. Bioeng.*, **25**, 26 (2008).
62. D. L. Yi, M. Yan, X. R. Qin, Z. W. Guan, L. L. Wang, Z. L. Xia and L. Wu, Spectrometric Analysis of the Complex Structure of Propyl Gallate-Iron, *Chin. J. Spectr. Lab.*, **25**, 833 (2008).
63. L. Wu, M. Yan, J. G. Wang, Z. L. Xia, X. R. Qin and D. L. Yi, Synthesis and Properties of Copper Complex with Propyl Gallate, *J. Wuhan Univ. Technol.*, **31**, 35 (2009).